PROCEEDINGS of the
23rd International Congress on Acoustics
9 to 13 September 2019 in Aachen, Germany

Model test stand for acoustic scattering

Wolfram Bartolomaeus[(1)]

[(1)]Federal Highway Research Institute, Germany, bartolomaeus@bast.de

Abstract

SCATTERING, DIFFRACTION and REFLECTION at an acoustical hard or soft obstacles affect the sound field in propagation. The scattering of sound waves on an acoustical hard cylinder was calculated analytically using a harmonic development according to Bessel functions, simulated with the finite element method (FEM) and measured in the Laboratory for Acoustic Modeling on a scaled level. A good agreement between all three results was found. Similarly, the diffraction of a sound pulse at an edge was analytically calculated using the theory of Biot, Tolstoy and Medwin (BTM) and simulated with an FEM model. These simulations and the room impulse response measured in the Laboratory also agree satisfactorily. For further measurements, the new Acoustic Scattering Model Test Stand (MPaS) can be used also for objects or sets of objects which no longer can be described analytically in an easy way. Likewise, measurements at diffraction edges and reflection planes are feasible. These can be compared with analytical solutions or at least with FEM simulations. Thus, the MPaS test stand provides an important tool for modeling the propagation of a sound field over obstacles, which makes it possible to construct e. g. optimized noise barrier attachments for roads in the future.

Keywords: Scattering, Diffraction, Biot-Tolstoy-Medwin, Simulation, Measurements

1 INTRODUCTION

Scattering, diffraction and reflection on acoustical hard or soft obstacles affect the sound field in propagation.

In this contribution the attempt is done to minimize the diffraction at the edge of a noise screen with the help of a special attachment, consisting of cylindrical scatters parallel to the edge.

After the description of scattering from one cylinder, and diffraction at an edge, considerations from the topic of acoustic crystals and refraction where taken to induce an optimization. After the calculation with the Finite–Element–Method (FEM) a model was measured at the model test stand for acoustic scattering (Modell–Prüftstand für akustische Streuung, MPaS) in the laboratory for acoustic model engineering (Halle für akustische Modelltechnik, HaMt).

2 SCATTERING AT A CYLINDER

2.1 Theory

It is possible to evaluate scattering at a cylinder analytically [1], [2].

For the cylindrical sound field the scattered pressure field is the sum of BESSEL functions J and HANKEL functions of the second kind $H^{(2)}$

$$p_s(r\phi) = P_0' \sum_{m=0}^{\infty} A_m' \delta_m J_m(kr_Q) H_m^{(2)}(kr) \cos(m\phi) \tag{1}$$

with

- P_0', source strength per unit length,
- k, wave index k,
- r_Q, radial distance to source r_Q,
- x, distance x–direction $x = r\cos\phi$ (with radial distance, r, and angle towards x–axis), ϕ, and
- $\delta_m = \begin{cases} 1; & m = 0 \\ 2; & m > 0 \end{cases}$.

The coefficiens A'_m are calculated from the ones of the scattering field with plan waves A_m

$$A'_m = \frac{H_m^{(2)}(kr_Q)}{J_m(kr_Q)} i^{-m} A_m. \tag{2}$$

For an acoustically hard cylinder with radius a the coeffiziens A_m are

$$A_m = -i^{m+1} e^{-i\gamma_m} \sin(\gamma_m). \tag{3}$$

Here γ_m is the phase angle

$$\gamma_m = \arctan\left(\frac{N_{m+1}(ka) - N_{m-1}(ka)}{J_{m+1}(ka) - J_{m-1}(ka)}\right). \tag{4}$$

2.2 FEM simulation

Scattering of acoustic harmonic waves at an acoustically hard cylinder were calculated analytically by expanding of BESSEL functions, simulated with a FEM model and measures in the HaMt.

The FEM model used was three dimensional but flat (s. Figure 1, left). In the right side of Figure 1 the total

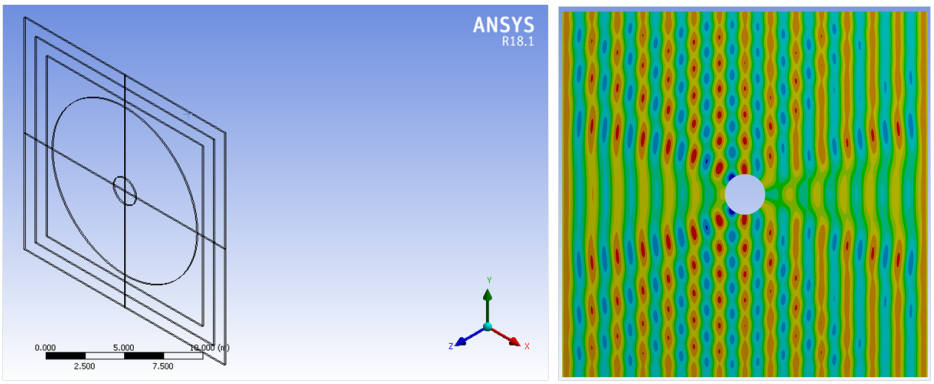

(a) FEM model and ... (b) ... total field.

Figure 1. Geometry of the used FEM model and total field of the scattering at an acoustically hard cylinder.

field of a plane wave with incident from the left is shown. From this the scattering field can be calculated.

2.3 Measurement

The measurement were taken at a hollow polycarbonate cylinder, 1 m long. The outer radius was 2 cm. The measurements were conducted with a two channel FFT measuring system. With this the transfer functions — and through Fourier transform (FFT) — the frequency spectra were measured (s. Figure 2, left).

On the right side of Figure 2 the results of the analytically calculation, the FEM simulation and the measurements in the HaMt for a frequency of 13.5 kHz (parameter $ka = 5$) are shown. All results are in a good agreement, but the measurements for large angles above $\pm 60°$.

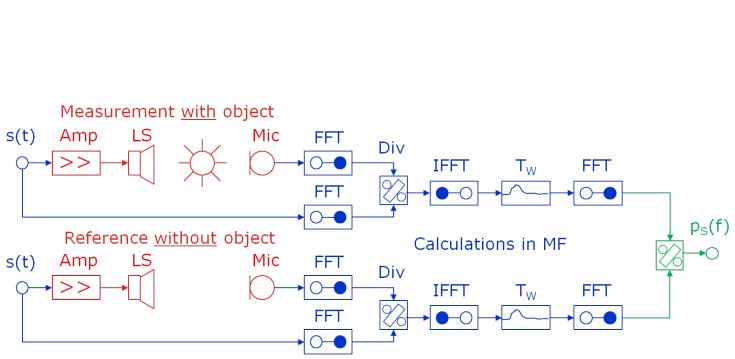

(a) Two channel FFT measurements — principal figure.

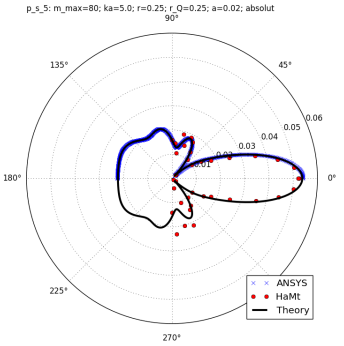

(b) Scattering at an acoustically hard cylinder — Comparison of theory, simulation (ANSYS) and measurements (HaMt).

Figure 2. Principle of measurements and results for scattering.

3 DIFFRACTION AT AN EDGE

3.1 Theory

KIRCHHOFF integral

Diffraction at an edge is typically solved for harmonic waves. The calculation of diffraction is done with the KIRSCHHOFF diffraction integral

$$u_P = -a_Q \cdot \frac{ik}{2\pi} \int\int \frac{e^{ik(r+r_0)}}{r \cdot r_0} \left[\frac{\cos\theta - \cos\theta_0}{2} \right] d\sigma \tag{5}$$

with

— a_Q, amplitude of the source,
— $k = 2\pi/\lambda$, absolute value of the wave vector,
— λ, wave length and
— $(\cos\theta - \cos\theta_0)/2$, slope factor.

The integral is to be taken over the area of the opening of the blind. The angles θ and θ_0 are situated between the outer normal of the area of the opening and the line from the receiving point P with length r and between the line from the source point Q with length r_0 to the opening respectively.

For a divergent point source the FRESNEL diffraction integral is

$$u_P = A \cdot (C + iS) \tag{6}$$

with

— $A = -a_Q \cdot \frac{ik}{2\pi} \cos\delta \frac{e^{ik(r+r_0)}}{r \cdot r_0}$,
— $C = \int\int \cos(k \cdot \Phi(\xi,\eta))\, d\xi d\eta$ and
— $S = \int\int \sin(k \cdot \Phi(\xi,\eta))\, d\xi d\eta$.

The angle δ is situated between the connection line from source point, Q, to receiving point, P, and the normal vector of the blind opening.

In the case, the integration area is a paraxial rectangle the integration variables can be separated. Here the FRESNEL integrals appear

$$U(w) = \int_0^w \cos\left(\frac{\pi}{2}u^2\right) du, \tag{7}$$

$$V(w) = \int_0^w \sin\left(\frac{\pi}{2}u^2\right) du. \tag{8}$$

They can be calculated numerically.

BIOT–TOLSTOY–MEDWIN

There is also an alternative way for calculating the diffraction from an edge. In the theory of BIOT–TOLSTOY–MEDWIN (BTM) [3] the impulse response (IR) for a geometrical configuration of obstacles is calculated. For this task the normal co-ordinates of the LAGRANGE formalism of the classical mechanic is used. The result are transient functions in time. We can calculate the diffraction at a wedge which can be specialised to the diffraction of an edge easily.

The temporal sequence of the sound pressure coming from a point source is [4]

$$p(t) = -\frac{S\rho c}{8\pi\Theta_W} \cdot \frac{1}{r_S r_R \sinh(\eta)} \cdot \sum_{i=1}^{4} \beta_i \tag{9}$$

with

- S, source strength (volume per time) flow staring at time $t = 0$; correspondent to a DIRAC delta function,
- ρ, density of the media (air),
- c, sound velocity (in air),
- Θ_W, edge angle,
- r_S, radial co-ordinate of the source,
- r_R, radial co-ordinate of the receiver,
- η, auxiliary quantity and
- β_i, absolute vales of the four angles.

The auxiliary quantity η consists of the geometry of the wedge

$$\eta = \cosh^{-1}\left[\frac{c^2t^2 - \left(r_S^2 + r_R^2 + z_R^2\right)}{2r_S r_R}\right] \tag{10}$$

with the distance between source and receiver along the edge, z_R (here we set $z_R = 0$).

The contribution of the four angles $\phi_i = \pi \pm \Theta_S \pm \Theta_R$ (with signs $++ : i = 1$, $+- : i = 2$, $-+ : i = 3$ and $-- : i = 4$) are

$$\beta_i = \frac{\sin(\nu\phi_i)}{\cosh(\nu\eta) - \cos(\nu\phi_i)} \tag{11}$$

with the wedge index, $\nu = \pi/\Theta_W$.

In Figure 3 the sound pressure for six angles of radiation β (definition see below) with dependency of time is shown.

For positive angles of radiation the sound pressure is positive, but decreasing with increasing angle of radiation. For negative angles of radiation the sound pressure is also negative, and also decreasing with increasing angle of radiation. At $\beta = 0^\circ$ the sound pressure is at least positive.

3.2 FEM simulation

In time domain FEM calculations are conducted. The model was three dimensional but flat and consists of about 1 mio. elements and 212 time steps. Die element length was 1 mm, the length of each time step 1,417 μs. In Figure 4 the sound field after 1,427 ms is shown.

At time $t = 0$ s an delta double impulse was created at the source point S1 (see below).

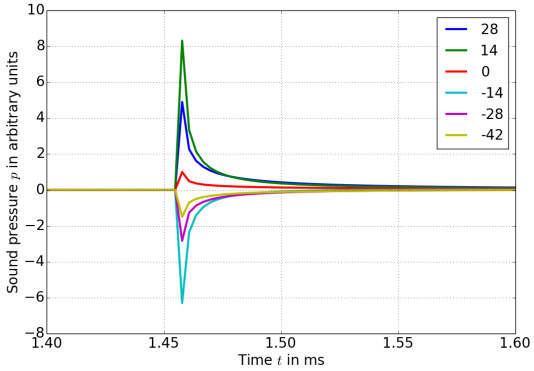

Figure 3. Diffraction at a reflection halve plane.

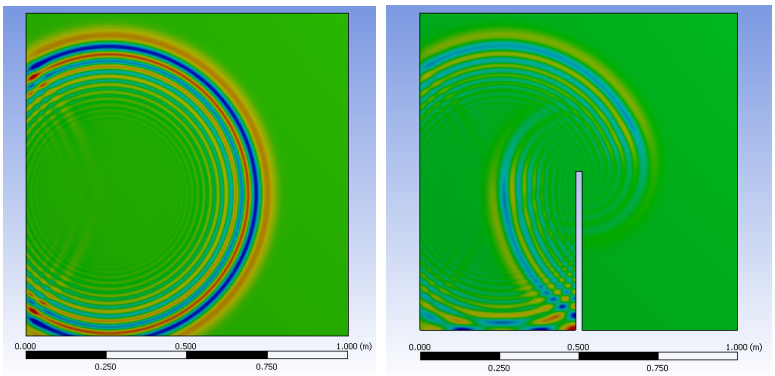

(a) Without ... (b) ... and with edge.

Figure 4. Sound field after 1.427 ms.

4 Model for an added device

4.1 Geometry

The model geometry of source, wall and receiver is taken from the norm draft for in situ measurements of sound diffraction [5]. Here we uses the low source position S1 which is 2.00 m in front of the reference plan of the wall (center line) and 0.50 m below the top edge. For a standard wall, 4.00 m high, the source position is 14.00 m in front of the wall, 0.50 m above the road surface. For the receiver the middle microphone position M3 is used which is 2.00 m behind the reference plan in the height of the top edge. In Figure 5 a sketch of use geometry is shown.

The incidence angle of the sound relative to the normal vector of the wall is $\alpha = 14°$.

If some scattering bodies are forming a periodic grad, methods of solid state physics are applicable. Here the scattering bodies are cylinders, arranged in parallel to the top edge of tghe wall, forming a two dimensional crystal.

Constructive interference occur at reflections on a crystal at the BRAGG condition

$$m\lambda = 2d\sin(\theta) \tag{12}$$

with

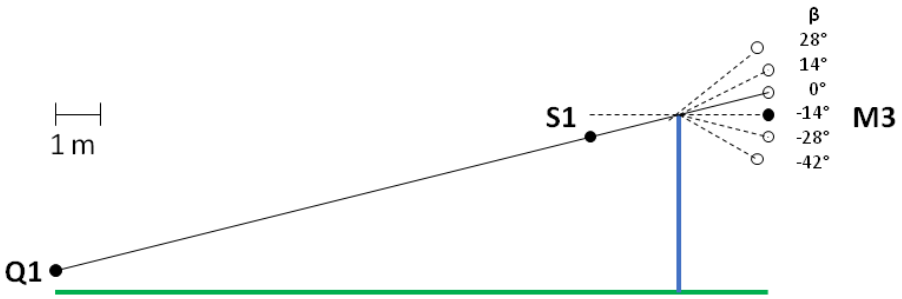

Figure 5. Geometry of source, wall and receiver.

— m , order of the reflection,
— λ, wave length,
— d, distance between two grid planes and
— θ, BRAGG angle.

For a square grid the grid constant L the 1st order of reflection occurs at a BRAGG angle of $\theta = 90°$ (perpendicular sound incidence, crystallographic direction ΓX) at the fundamental BRAGG resonance frequency

$$f_{\Gamma X} = \frac{c}{2\lambda} \tag{13}$$

with sound velocity, c $(= \lambda f)$.

At the fundamental BRAGG resonance frequency the transition through the crystal is small, it has got a high sound insulation. There is good sound transition at three times the fundamental BRAGG resonance frequency. At this frequency the reflection is small [7].

Die Idea is to cause a sound deceleration in this frequency range. Then an destructive interference between the sound diffracted over the crystal and the sound transmitting through the crystal will take place.

For this reason we firstly calculate the refraction index of the crystal n, depending of the filling fraction [8]

$$n = \sqrt{1 + \frac{\pi}{2}\left(\frac{r}{d}\right)^2} \tag{14}$$

with the radius of the cylinder, r.

Destructive interference occurs at a difference in path length of $\lambda/2$. The necessary width of the crystall B is therefore

$$B = \lambda \cdot \frac{1}{2(n-1)}. \tag{15}$$

A deflection of the sound ray can be achieved by a suitable form of the crystal. At a prismatic form the angle of the refraction edge, θ, can be calculated in dependence of the incident angle, α, and the refraction index, n

$$n = \frac{\sin\left(\frac{\alpha+\theta}{2}\right)}{\sin\left(\frac{\theta}{2}\right)}. \tag{16}$$

The Idea of an added device with cylinders forming a crystal was realised at the MPaS. Tubes of aluminium with a length of 1 m an a radius of $r = 3$ mm are forming a square grid with a grid constant of $d = 7$ mm. The BRAGG frequency is $f_{\Gamma X} = 24$ kHz with a wave length of $\lambda = 14$ mm. The refraction index for this arrangement is $n = 1.135$ (14). The calculated width is $B = 52$ mm (15) resulting of a horizontal number of 7 to 8 cylinders. To make sure the added device is "visible", a minimum height of several wavelength is required. With a vertical number 4 cylinders the height is 2λ. From the prism equation, (16), the optimum angle for the prism is $\theta = 81°$. For a square crystal this is almost fulfilled.

4.2 Measurements at the model stand

In Figure 6 the MPaS with the added device is shown. On the left a 4–PI loud speaker can be seen — a ribbon tweeter with a Frequency range of 2 kHz to 40 kHz. On the right a 1/4" microphone fixed at the turning table is visible.

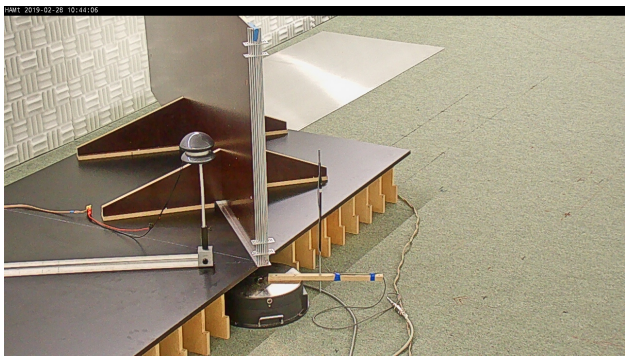

Figure 6. MPaS with added device.

The microphone is turning centrically in steps of 14° around the edge of the wooden plate. The shadow boarder is defined at an angle of $\beta = 0°$. For higher angles the microphone is in the shadow, at lower —respectfully at angles above 360° — there is a visible relation between loud speaker an microphone.

4.3 Results and discussion

The sound diffraction at the edge of a wall can be calculated for different radiation angles β as a function of frequency. In Figure 7, on the left, the sound level degression as a function of the logarithm of the frequency is shown. Measurements are in solid lines, FEM simulations at a 20 mm thick wall in circles and a calculation at a non reflecting halve plane dashed.

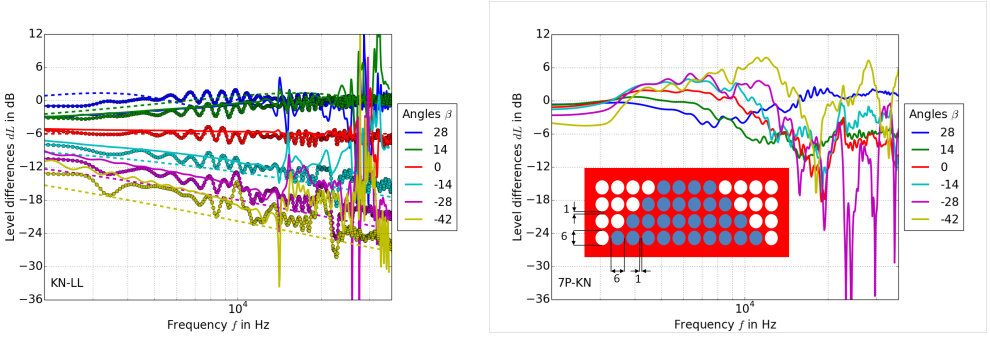

(a) Diffraction at an edge. Measured (solid line), simulated (circles) and calculated (dashed).

(b) Measured sound level difference added between added device and edge.

Figure 7. Diffraction at a pure edge and difference between device and edge.

The conformity of measurements and calculations is satisfying. At the shadow boarder at $\beta = 0°$ the sound insulation is $dL = 6$ dB as expected. At higher angles — above the shadow zone — the sound insulation of the wall gets lost. A characteristic wave figure around sound difference of 0 dB can be seen. At lower angles — in the shadow zone — the sound insulation is increasing. The efficiency for higher frequencies is increasing rapidly — about 10 dB per octave.

In Figure 7, on the right, the measured sound level difference between wall with added device and wall without added device is drawn for frequencies of 2 kHz to 36 kHz.

The geometry of the added device is drawn as a cross section. In this case the added device consists of 28 cylinders.

The acoustical effectiveness begins at about 10 kHz. At an angle of $\beta = 0°$ the increase in level is less than 2 dB at about 4 to 7 kHz. But the collapse is up to 18 dB at about ca. 20 kHz. At larger angles, i. e. in the shadow zone, an increase in level of about 6 dB is noticeably, but the collapse is at least as strong as for the horizontal radiation angle. For $\beta = -28°$ it is even more significant. At the shadow boarder at $\beta = 14°$ no increase in level takes place. But the collapse is about 10 dB less. For even higher sound rays ($\beta = 28°$) the level difference is very small.

For an optimised shielding effect of sound emissions from roads a scale of 1:10 to 1:16 is required.

REFERENCES

[1] Morse, Ph. M.; Ingard, K. U. Theoretical Acoustics. Princeton university, Princeton 1986.

[2] Mechel, F. P. Formulas of Acoustics, Springer Verlag, Berlin 2008.

[3] Tolstoy, I. Wave Propagation, McGraw–Hill, New York 1973.

[4] Calamia, P. Th. Advances in Edge–Diffraction Modeling for Virtual–Acoustic Simulations, Dissertation 2009.

[5] FprEN 1793–4:2014 (D) Lärmschutzvorrichtungen an Straßen — Prüfverfahren zur Bestimmung der akustischen Eigenschaften — Teil 4: Produktspezifische Merkmale — In–situ–Werte der Schallbeugung; Deutsche Fassung FprEN 1793–4:2014.

[6] DIN ISO 9613–2 Dämpfung des Schalls bei der Ausbreitung im Freien — Teil 2: Allgemeines Berechnungsverfahren (ISO 9613–2 : 1996).

[7] Chong, Y. B. Sonic Crystal Noise Barriers, PhD thesis The Open University 2012.

[8] Meyer, E.; Neumann, K.–G. Physikalische und Technische Akustik, Vieweg, Braunschweig 1979.